DEVELOPMENT OF A TRANSIENT, MULTI-FEED GEOTHERMAL WELLBORE SIMULATOR

Ryan Tonkin[1], John O'Sullivan[1] and Michael O'Sullivan[1]

[1] Department of Engineering Science, University of Auckland, Auckland, New Zealand

rton671@aucklanduni.ac.nz

Keywords: *wellbore, multi-feed, transient, two-phase, simulation, validation*

ABSTRACT

Simulation of the flow in a geothermal wellbore is an important reservoir engineering task, but most existing geothermal wellbore simulators can only deal with steady-state conditions. This paper discusses the theoretical background of a transient geothermal wellbore model that is currently under development. The simulator is capable of modelling transient single and two-phase flow in wells with multiple feed-zones. A geothermal wellbore simulator solves the conservation of mass, momentum and energy equations governing the flow in a geothermal wellbore. These, along with the additional equations required for model closure, are presented. These governing equations are discretised and solved numerically using the Newton-Raphson procedure. The simulator is tested using analytical solutions for simplified single-phase flow situations. Steady-state validation cases are presented for both single-feed and multi-feed wellbores and a simulation of the transient behaviour of a geothermal production well is presented as a test case. Finally, further applications of the simulator are discussed.

1. INTRODUCTION

Wells play a critical role in the exploitation and management of geothermal systems. They form the link between the subsurface geothermal system and the energy production facilities on the surface. The direct monitoring and analysis of geothermal wellbores provides vital information about their behaviour (Axelsson, 2013). However, the harsh operating conditions, as well as the expense and complexity of running flowing surveys in geothermal wells, often prevent the installation of measuring equipment (Upadhyay et al., 1977). Therefore, geothermal wellbore models provide an invaluable tool for inferring the characteristics of geothermal wellbores and predicting their future behaviour.

Many steady-state wellbore models exist, e.g., HOLA (Bjornsson, 1987; Aunzo et al., 1991), WELLSIM (Gunn and Freeston, 1992), SWELFLOW/SIMGWELL, (McGuiness, 2015; Marquez et al., 2015), FLOWELL (Gudmundsdottir and Jonsson, 2015). However, there are only a few applications of transient geothermal wellbore simulation. For example, some of the transient processes associated with output tests were studied by simulation (Miller, 1980a; Miller et al. 1982; Khasani et al., 2017). Recently, transient simulations were used to investigate the impact of multiple feeds on production testing of geothermal wells (Vasini et al., 2018) using T2WELL (Pan et al., 2011), well cycling (Yamamura et al. 2016; Yamamura et al., 2017, Itoi et al. 2013) and airlifting during wellbore startup (Akbar et al., 2016).

This study describes the theoretical background and implementation of a new transient wellbore simulator. Multi-phase fluid flow in a geothermal wellbore is governed by three fundamental laws: conservation of mass, conservation of momentum and conservation of energy. These are presented in Section 2 along with the additional constitutive equations required for model closure. The verification and validation of the simulator against simple analytical solutions and flowing pressure-temperature logs is presented in Sections 3 and 4, respectively. Finally, a simulation of the transient behaviour of a multi-feed well is discussed in Section 4.

2. MATHEMATICAL MODEL FORMULATION

The equations governing flow in a geothermal wellbore, representing the conservation of mass, momentum and energy within a wellbore element, are discussed in Section 2.1. The constitutive models required for closure are presented in Section 2.2. In our simulator these equations are discretised and solved implicitly using a multi-variate Newton-Raphson procedure. The primary variables are pressure, temperature (saturation in two-phase), vapour velocity and liquid volume flux. The discrete model is not presented here, instead it is discussed in a companion paper (Tonkin et al., 2020).

2.1 Two-phase conservation equations

The governing equations for the three-equation model for fluid flow in a deviated geothermal wellbore, with a variable cross-sectional area are given by (1), (2) and (3) below (Yadigaroglu and Hewitt, 2018). They describe the behaviour of the fluid as a mixture rather than dealing with each phase individually, however the equations are written in terms of separate quantities for each phase. This formulation ensures that effects of phase slip on momentum and energy transport are accounted for. The assumptions on which this model is based are:

- 1-D flow – flow variables are averaged across the well cross-section;
- equal pressure in each phase;
- negligible axial heat conduction;
- the two phases are in local thermodynamic equilibrium; and
- a relationship between the velocities of liquid and gas (slip relationship).

The effects of non-condensable gases and dissolved salts are not considered here but could be included by adding additional conservation equations.

The conservation of mass for a two-phase mixture can be written as

$$\frac{\partial}{\partial t}[\rho_v S_v + \rho_l S_l] + \frac{1}{A}\frac{\partial}{\partial s}[A\rho_v S_v u_v + A\rho_l S_l u_l] - q_{mass} = 0. \quad (1)$$

ISSN 2703-4275

Here the subscripts *l* and *v* are used for the liquid and vapour phases, respectively. The saturations are given by S_l and S_v, u_l and u_v are the velocities and ρ_l and ρ_v are the densities. The independent variable *s* is the distance up the wellbore, *A* is the cross-sectional area of the well and external sources of mass (e.g. reservoir feed-zones) are given by q_{mass}.

The equation governing conservation of momentum is

$$\frac{\partial}{\partial t}[\rho_v S_v u_v + \rho_l S_l u_l] + \frac{1}{A}\frac{\partial}{\partial s}[A\rho_v S_v {u_v}^2 + A\rho_l S_l {u_l}^2] + \frac{\partial P}{\partial s} + \frac{2}{r}\tau + (\rho_v S_v + \rho_l S_l) g \frac{\partial z}{\partial s} - q_{mom} = 0. \quad (2)$$

Here, *P* is the wellbore pressure, *g* is gravitational acceleration and τ is the wellbore friction term. The variable *r* is wellbore radius and *z* is the vertical elevation. The external source or sink of momentum is given by q_{mom}.

The conservation of energy equation is

$$\frac{\partial}{\partial t}\left[\rho_v S_v \left(h_v + \frac{1}{2}{u_v}^2\right) + \rho_l S_l \left(h_l + \frac{1}{2}{u_l}^2\right) - P\right] + \frac{1}{A}\frac{\partial}{\partial s}\left[A\rho_v S_v u_v \left(h_v + \frac{1}{2}{u_v}^2\right) + A\rho_l S_l u_l \left(h_l + \frac{1}{2}{u_l}^2\right)\right] + (\rho_v S_v u_v + \rho_l S_l u_l) g \frac{\partial z}{\partial s} + q_{heat} - q_{ener} = 0. \quad (3)$$

Here it is given in terms of the enthalpy and kinetic energy of each phase. The term, q_{heat} is the heat flux away from the wellbore into the formation due to conduction and q_{ener} represents the energy injected or produced by sources or sinks. The enthalpies of the phases are given by h_v and h_l.

2.2 Constitutive equations

Equations (1), (2) and (3) have more unknowns than the number of conservation laws and supplementary constitutive equations are required to complete the set of equations. There is a wide range of constitutive models to choose from and the selection made has a significant impact on simulation results (Akbar et al, 2016). The constitutive models for phase slip, heat flux, friction and source terms are discussed below.

2.2.1 Phase slip

Modelling multi-phase fluid flow with a single mixture momentum equation requires an additional constitutive equation to model the "slip" between the phases. Slip describes the tendency for vapour to have a higher velocity than liquid in two-phase flow due to buoyancy effects. The drift flux formulation of slip is used in our simulator. Other common slip models are discussed by Vijayan et al. (2000).

Zuber and Findlay's (1965) drift flux model for slip is

$$u_v = C_0 F_V + u_d. \quad (4)$$

It relates the velocity of the vapour phase to the total volume flux of the fluid mixture. Here, F_V is the total volume flux (often represented by the symbol *j*), also called the velocity of the centre of volume, and is defined as

$$F_V = S_v u_v + S_l u_l. \quad (5)$$

The mean drift velocity, u_d, is the velocity of the vapour phase relative to the volumetric flux of the two-phase mixture and C_0 is the shape factor (also called the distribution parameter). Empirical equations are required for both u_d and C_0. Homogeneous flow is the simplest model for slip. It assumes no slip between the phases, meaning the phase velocities are equal, i.e. $u_l = u_v$. Homogeneous flow can be represented by the drift-flux model with $u_d = 0$ and $C_0 = 1$.

The drift flux model we use is the same as that used by Pan et al. (2014) (adapted from Shi et al. (2005)). It has been shown to produce good results in geothermal applications (Vasini et al. 2018; Pan et al., 2015). However, the choice of the slip relationship has a large effect on the results of wellbore simulation (García-Valladares et al., 2006) and further research is required into the best slip relationship for modelling the transient behaviour of geothermal wells. Our simulator is written in a general form and can easily be modified to include other slip models.

2.2.2 Wellbore friction

A constitutive equation is required for modelling the friction force between the geothermal fluid and wellbore wall. A two-phase form of the classical Darcy–Weisbach equation is used:

$$\frac{2}{r}\tau = \frac{1}{4r} f F_m \left|\frac{F_m}{S_v\rho_v + S_l\rho_l}\right|. \quad (6)$$

Here the total mass flux, F_m, is defined as

$$F_m = S_v\rho_v u_v + S_l\rho_l u_l. \quad (7)$$

The Darcy friction factor, *f*, is a function of the Reynold number (Re) and the pipe roughness and is calculated using the Colebrook-White equation. The two-phase Reynolds number is calculated as

$$Re = \frac{F_m d}{S_v\mu_v + S_l\mu_l}, \quad (8)$$

where *d* is the well diameter and μ_v and μ_l are the dynamic viscosities of the vapour and liquid phases.

This model for friction was chosen for both its simplicity and because it varies smoothly across all phase states. Additionally, it has been used in transient geothermal models by Pan et al. (2014) and Akbar et al. (2016). Older transient simulators (Miller 1980; Garcia-Valladares et al., 2006) have calculated friction losses using "two-phase multiplier" methods. This method multiplies the single-phase version of (6), calculated with the properties of the liquid phase, by an empirical term (Chisholm, 1973; Beattie, 1973).

2.2.2 Wellbore heat loss

The heat loss from the wellbore to the reservoir due to conduction, q_{heat}, is modelled using Ramey's equation for heat loss (Ramey, 1962, Horne and Shinohara, 1979),

$$q_{heat} = \frac{2}{r}\frac{k_{res}U(T_{wb} - T_{res})}{k_{res} + rUf(t_D)}. \quad (9)$$

Here, the dimensionless time is defined as $t_D = \alpha t / {r_c}^2$ where $\alpha = k_{res}/\rho_{res}c_{res}$ and r_c is the radius of the cement-reservoir interface, and k_{res}, ρ_{res} and c_{res} are the thermal conductivity, density, and specific heat capacity of the reservoir. T_{res} is the formation temperature, T_{wb} is the wellbore temperature and *U* is the over-all heat transfer coefficient. The time function, $f(t_D)$, approximates the transient nature of wellbore-formation heat exchange. Chiu and Thakur's (1991) version of the time function is given by:

$$f(t_D) = 0.982 \ln(1 + 1.81 t_D). \quad (10)$$

This formula has been shown to provide a reasonable approximation of transient wellbore-reservoir heat exchange

ISSN 2703-4275

(Vasini et al., 2018) while avoiding the early time discontinuity that results from using Ramey's (1962) original time function.

Willhite (1967) provided a general expression for the term U in (9), that describes the thermal resistance of any wellbore completion. For the present study Willhite's (1967) equation was simplified to only include the effects of a single cemented annulus, and thus

$$U = \frac{k_c}{r\,ln(r_c/r)}. \quad (11)$$

Here, k_c is the thermal conductivity of the cement, r is the wellbore radius and r_c is the radius of the cement-reservoir interface.

2.2.3 Source terms

The source terms q_{mass}, q_{mom} and q_{ener} in (1), (2) and (3) describe the mass, momentum and energy transfer between the reservoir and wellbore. The total mass source is the sum of the liquid and vapour components,

$$q_{mass} = q_{mv} + q_{ml}. \quad (12)$$

The reservoir mass source for each fluid phase, $q_{m\beta}$, is calculated using a deliverability equation based on two-phase Darcy flow:

$$q_{m\beta} = \frac{k_{r\beta}}{\nu_\beta}\mathrm{PI}(P_{res} - P_{wb})/V. \quad (13)$$

Here, $k_{r\beta}$ and υ_β are the relative permeability and kinematic viscosity of each phase, P_{res} is a prescribed reservoir pressure, and $V=\pi r^2\Delta s$ is the volume of the wellbore element. Combining (12) and (13), the total mass input can be written in term of a lumped parameter, α:

$$q_{mass} = \alpha(P_{res} - P_{wb})/V. \quad (14)$$

The energy source in (3) is modelled as

$$q_{ener} = q_{mass}h_{fres}, \quad (15)$$

in which h_{fres} is the flowing enthalpy of the feed,

$$h_{fres} = \frac{\frac{h_l k_{rl}}{\nu_l} + \frac{h_v k_{rv}}{\nu_v}}{\frac{k_{rl}}{\nu_l} + \frac{k_{rv}}{\nu_v}}. \quad (16)$$

Here, h_l and h_v are the reservoir enthalpies.

Finally, the fluid from the feed is assumed to enter the well perpendicular to the direction of flow (Bendikson et al., 1991). As such, there is no net transfer of momentum meaning $q_{mom} = 0$ in (2).

2.2.4 Thermodynamic properties

The properties of pure water are calculated using the revised IAPWS industrial formulation 1997 (2007). The surface tension is calculated using the IAPWS revised correlation (2014).

3. MODEL VERIFICATION

Analytical solutions can be derived for simplified forms of the single-phase conservation equations and these are used to check the numerical implementation of the simulator.

3.1 Test 1 – Constant density model

A simple linear model is derived by assuming steady-state flow of a single-phase isothermal fluid. The fluid density and frictional effects are assumed to be constant. Applying these assumptions to (1) and (2) and integrating with respect to pressure gives

$$P(z) = P_0 - z\left(\frac{f}{4r}\frac{F_m|F_m|}{\rho} + \rho g\right). \quad (17)$$

Here, P_0 is the wellhead pressure. The coefficient of friction, f, was fixed at 2.5E-2. Simulations were run for both liquid and vapour conditions in a 1500 m vertical wellbore with a diameter of 0.216 m, discretised into 10 elements. A constant wellhead pressure of 8 bar was use while the mass flux on the bottom boundary was varied. Figures 1 and 2 show a good match between the analytical model and numerical results for a variety of mass flow rates. Although simple, this solution helps to verify that the implementations of the gravitational and friction terms are correct.

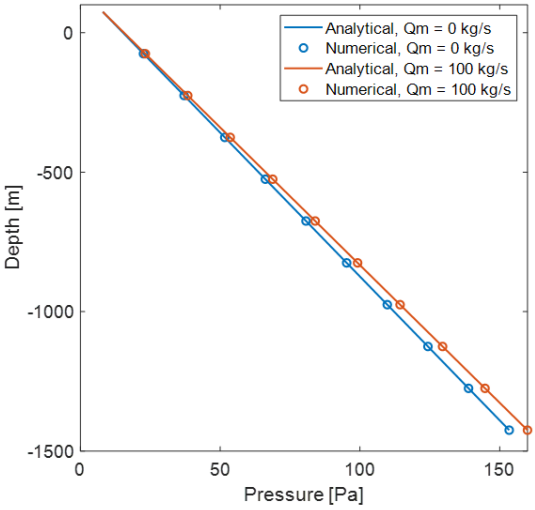

Figure 1: Comparison of numerical and analytical solutions for test case 1 for single-phase liquid

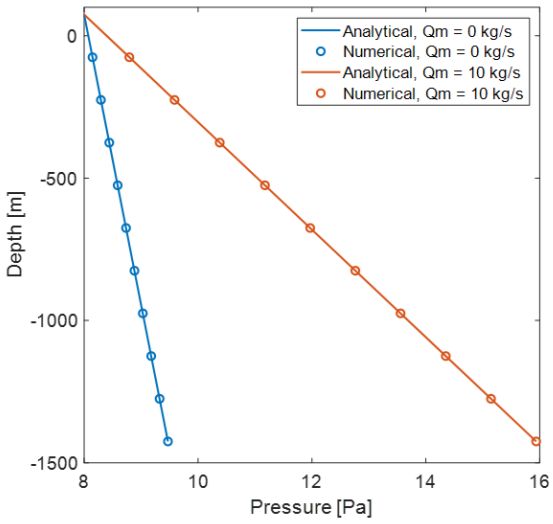

Figure 2: Comparison of numerical and analytical solutions for Test Case 1 for single-phase vapour

3.2 Test 2 – Linear density model

A second simple analytical solution was derived for a steady-state, single-phase isothermal fluid. The fluid density is assumed to be a linear function of pressure, such that $\rho = mP + c$, derived from the IAPWS-IF97 correlations, and friction effects are ignored. This is a simplified case of a semi-analytical solution presented by Pan et al. (2011). The following equation for the wellbore pressure gradient results from simplifying (1) and (2) using these assumptions.

$$\frac{dP}{dz} = -\frac{\rho g}{{F_m}^2 \frac{d}{dP}(1/\rho)+1}, \tag{18}$$

Inverting (18) and integrating with respect to pressure gives an analytical expression for depth in terms of wellbore pressure,

$$z(P) = C - \frac{1}{mg} ln\,|\,\rho| - \frac{{F_m}^2}{2g}\frac{1}{\rho^2}, \tag{19}$$

where,

$$C = \frac{1}{mg} ln\,|\,\rho(P_0)| + \frac{{F_m}^2}{2g}\frac{1}{\rho(P_0)^2}. \tag{20}$$

Here, $\rho(P_0)$ is the density calculated from the wellhead pressure, and m is the gradient of density with respect to pressure. The lengths of the wellbores were 4000m and 1500m for the liquid and vapour simulations, respectively. Both were discretised into 50 elements. Figure 3 presents the comparison between the analytical and numerical solutions for liquid water flowing at 20 kg.m^{-2}.s^{-1}.

A good match is achieved with a maximum relative error of 0.03% between the analytical and numerical depths. Changes in mass flux have little influence on the pressure profile due to the low compressibility of water and have not been presented.

Figure 4 compares the analytical and numerical solutions for the vapour case, at two flow rates. A good match is achieved for both cases with maximum percentage errors of 0.07% and 0.4% for the 20 kg.m^{-2}s^{-1} and 400 kg.m^{-2}s^{-1} cases, respectively.

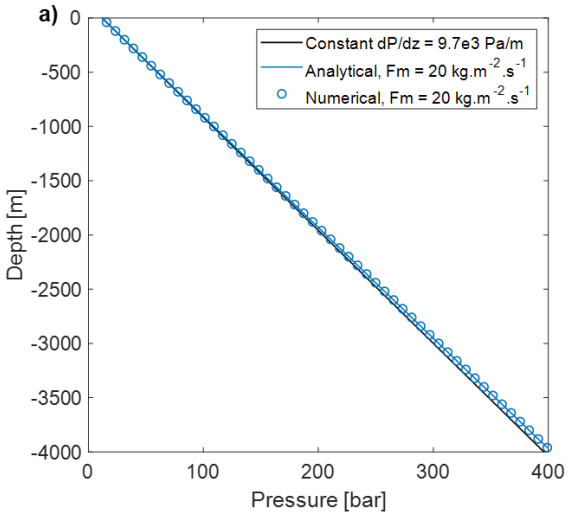

Figure 3: Comparison of numerical and analytical solutions for Test Case 2 for single-phase liquid

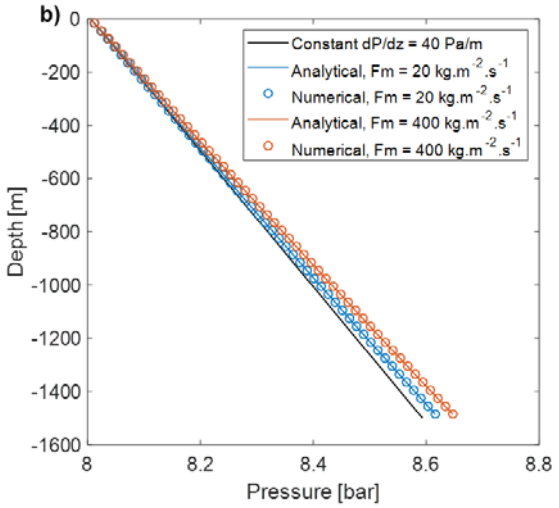

Figure 4: Comparison of numerical and analytical solutions for Test Case 2 for single-phase vapour

3.3 Test 3 – Ramey's solution for wellbore heat transport

Ramey (1962) presented an analytical approximation for wellbore temperatures during steam injection. Ramey's method was presented for geothermal applications by Horne and Shinohara (1979) for both production and injection cases. This method assumes the fluid has a constant density and constant heat capacity and that it is flowing at a steady rate. The reservoir was assumed to be radially symmetric and to have a constant vertical temperature gradient.

Both liquid and vapour simulations were run with a reservoir thermal conductivity (k_{res}) of 2.422 W.m^{-1}.K^{-1} and an overall heat transfer coefficient *(U)* of 20 W.m^{-2}K^{-1}. Chiu and Thakur's (1991) time function, given in (10), was used.

All simulations were run with a wellhead pressure of 8 bar at 0 kg.m^{-2}.s^{-1}, 50 kg.m^{-2}.s^{-1} or 350 kg.m^{-2}.s^{-1} for 1.0E7 seconds. The bottom-hole temperatures were 175 °C and 300 °C for the liquid and vapour simulations, respectively.

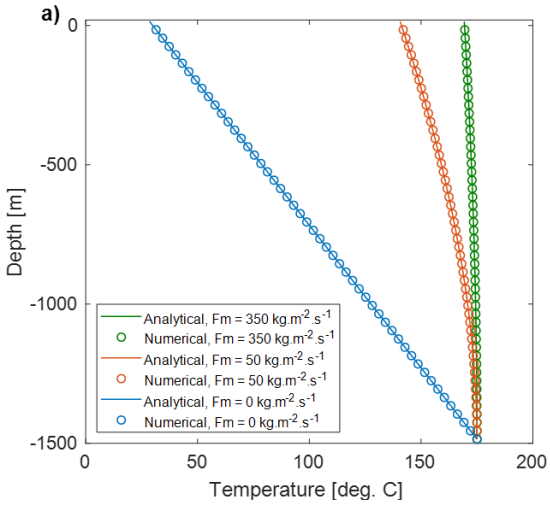

Figure 5: Comparison of numerical and analytical solutions for Test Case 3 for single-phase liquid

The reservoir temperature profiles varied linearly from 30 °C to 175 °C for the liquid cases and from 200 °C to 300 °C for the vapour cases. As expected, the wellbore temperature profile approaches the reservoir temperature profile for a closed well as shown by the cases of zero flowrate in Figure 5 and Figure 6.

The verification simulations matched the analytical solutions well. For liquid flow, given in Figure 5, the maximum difference between the analytical and simulated temperature values was 0.1% and 0.01% for the 50 $kg.m^{-2}.s^{-1}$ and 350 $kg.m^{-2}.s^{-1}$ cases, respectively. For vapour flow, given in Figure 6, the maximum difference was 0.08% and 0.01% for the 50 $kg.m^{-2}.s^{-1}$ and 350 $kg.m^{-2}.s^{-1}$ cases, respectively.

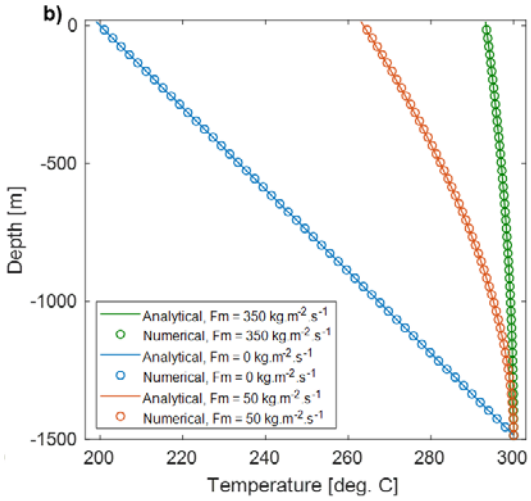

Figure 6: Comparison of numerical and analytical solutions for Test Case 3 for single-phase vapour

4. MODEL VALIDATION

Validation assesses the ability of the simulator to reproduce real-world observations. Two wells were chosen from the existing literature for validation simulations. Data for Well 6-1 from the East Mesa field in California was sourced from Ortiz-Ramirez (1983) and data for Well KJ-11 from the Krafla field in Iceland was sourced from Bjornsson (1987).

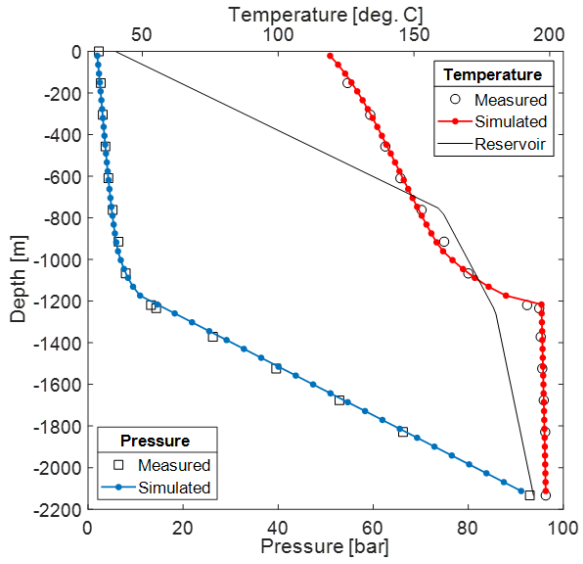

Figure 7: Comparison of pressure and temperature data with steady-state simulated profiles for East Mesa 6-1.

Well 6-1 is 2133 m deep with a uniform internal diameter of 0.2215 m. The well was discretised into 50 uniform elements. A bottom-hole pressure and temperature of 93 bar and 198.5 °C are used as boundary conditions in the bottom cell. The total mass flux is fixed at 335 $kgm^{-2}s^{-1}$ on the top boundary (wellhead). The shut-in wellbore temperature profile, given by Ortiz-Ramirez (1983), was used as a far-field reservoir temperature and is shown in Figure 7. The wellbore completion and reservoir are assumed to have an overall heat transfer coefficient of 20 $W.m^{-2}K^{-1}$ and a thermal conductivity of 2.422 $W.m^{-1}.K^{-1}$, respectively. Figure 7 shows that the simulated steady-state profiles for Well 6-1 match the experimental data well, with an average difference between the recorded and simulated pressures and temperatures of 5.6% and 0.69%, respectively.

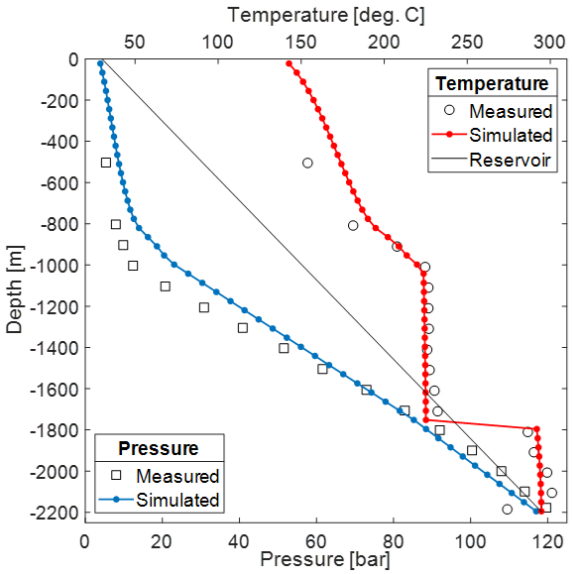

Figure 8: Comparison of pressure and temperature data with steady-state simulated profiles for Krafla KJ-11.

Well KJ-11 is a classic example of a well with multiple feed-zones, each with very different characteristics. Well testing indicated that feed-zones exist between 850-1050m, at 1500 m and below 1800m. Bjornsson (1987) presented several interpretations of the downhole data given in Figure 8. The case of influx from all feeds was chosen as a validation case. KJ-11 has a depth of 2217m with an internal diameter of 0.214m for the top 750m and an internal diameter of 0.177m from 750m to the bottom-hole. A linear geothermal gradient from 30-295 °C was assumed, as shown in Figure 8. An overall heat transfer coefficient of 20 $W.m^{-2}K^{-1}$ and thermal conductivity of 2.422 $W.m^{-1}.K^{-1}$ were used. A fixed mass flow of 30 kg/s was prescribed at the top boundary. The depth, mass flow and enthalpy of each feed, estimated by Bjornsson (1987), are given in Table 2.

Figure 8 presents the comparison between measured downhole data and the results of the simulation. The average difference between measured and simulated pressures was 27.8%. This is a results of an underestimated pressure gradient between 800 m and 1500 m. A good match has been achieved for the temperature profile with an average difference of 2.9% between the measured and the simulated values. These are deemed relatively good matches given the uncertainty in the conceptual model of the feed-zones in the well.

ISSN 2703-4275

Table 2: Reservoir source parameters

Name	Depth [m]	Mass flow [kg/s]	Enthalpy [kJ/kg]
Feed 1	840 - 930	7.80	670
Feed 2	1730 - 1770	21.0	950
Feed 3	2180 - 2220	1.20	1312

5. TRANSIENT MULTI-FEED EXAMPLE

The start-up process for a multi-feed well is presented here as an example of a transient geothermal wellbore simulation. The wellbore structure, including the location of feed-zones and numerical discretisation was taken from the KJ-11 validation example given in Section 4. The wellbore radius and feed-zone locations are shown in Figure 9 c) and the feed-zone parameters are given in Table 3 below. Here, α is a lumped productivity index calculated for use in (14). The pressure, enthalpy and productivity index assigned to each feed are artificial and do not represent the Krafla geothermal field. Instead, they were chosen to facilitate down-flow in the well.

Table 3: Source parameters for reservoirs

Name	Depth [m]	α [kg/s/Pa]	Pressure [bar]	Enthalpy [kJ/kg]
Feed 1	840 – 930	1.00E-06	95	770
Feed 2	1730 – 1770	3.20E-06	160	950
Feed 3	2180 – 2220	3.00E-07	185	1312

The initial state of the wellbore is given in Figure 9 below. The well has a small positive mass flow of 0.2 kg/s leaking from the wellhead and internal circulation between the feed-zones. Fluid enters the well at Feed 1 flowing both to the surface and down to Feeds 2 and 3. The initial wellbore temperature profile is significantly altered by this process and does not reflect the reservoir temperatures (a linear temperature profile between 30 and 295 °C).

Flow in the well is started by dropping the wellhead pressure from its initial values of 4.8 bar to a value of 2.5 bar. This value is held constant throughout the simulation. Zero velocity conditions are enforced on the bottom boundary and sources of mass and enthalpy vary based on the productivity indices provided in Table 3.

Figure 10 below shows profiles for pressure, temperature, saturation, and mass flow at various times during the simulation. After 10 minutes the increase in temperature at -1750m indicates production from Feed 2. At 2:45 hours, the temperature in the well has risen sufficiently for two-phase conditions to exist at the wellhead. Following this stage, the wellbore flashes rapidly due to the higher enthalpy fluid from Feed 2. Over the next 15-minute period, the well flashes along a length of approximately 650 m. During this flashing process, large changes in the overall fluid density cause a significant drop in wellbore pressures and a large increase in the total mass flow rate. By 5:00 h, steady-state conditions are reached.

Although the above problem is relatively simple, it demonstrates the ability of the simulator to model situations with fast changes in fluid properties occurring over large sections of the well. Additionally, it highlights the use of a transient simulator to study the interaction between major feeds and how this affects the mass flow rate and enthalpy of the production fluid. This has significant implications for situations where production or re-injection processes induce internal circulation between major feeds.

6. CHALLENGES FOR THE FUTURE

The understanding of key processes in geothermal engineering can be improved using transient wellbore simulations. Some examples are given below.

Transient well-test analysis infers reservoir characteristics from the measured pressure response due to changes in wellbore flow rate (Zarrouk and McLean, 2019). This transient pressure response is governed by a complex combination of reservoir and wellbore dynamics. Early investigations of well-testing using a wellbore simulator were completed by Miller (1980) and Miller et al. (1982), however, no further investigations have been completed. Although numerical reservoir simulations have been used to investigate

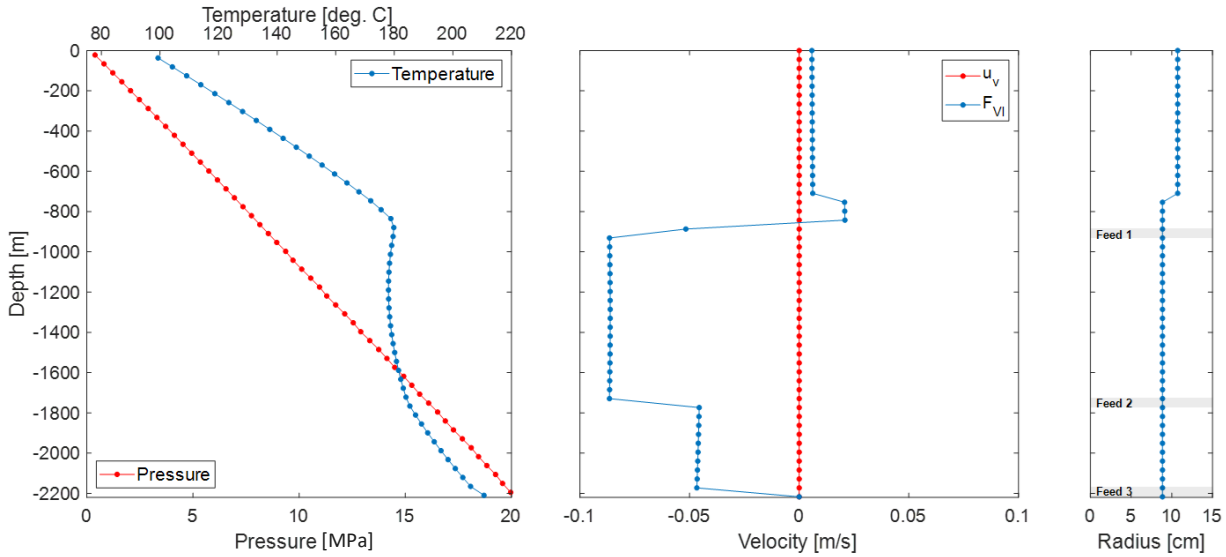

Figure 9: The initial conditions for pressure and temperature, liquid volume flux and vapour velocity. Internal circulation between the feeds is shown clearly in the velocity and temperature profiles.

these tests, the simulators used cannot account for complex well behaviour (e.g. internal flow between feeds). Transient coupled simulations are required to understand these processes further.

Completion tests involve injecting cold water into wells at different flow rates. Permeable zones are then identified from PTS logs taken during testing. Internal circulation between feeds can affect the interpretation of these tests (Zarrouk and McLean, 2019). Transient, fully coupled simulations of the wellbore-reservoir system will improve understanding of these effects and improve the interpretation of test results. A transient wellbore simulator with multi-feed and counter-flow capabilities is required to model these tests.

Well deliverability may change in response to reservoir conditions. This process has been investigated infrequently using coupled wellbore-reservoir models. However, it is unclear whether the pseudo-transient, loose-lagged coupling used in these investigations can adequately model these processes. Transient, coupled simulations can be used to validate or improve current methods.

7. CONCLUSION

This paper outlines the initial development and testing of a transient, multi feed-zone geothermal wellbore simulator. This included the presentation of the governing conservation equations, a clear statement of the assumptions made in their derivation and an explanation of the additional constitutive equations required for model closure. The simulator was verified against analytical solutions for very simple flows and validated against PT logs from both a single and multi-feed well. A test-case simulation that modelled the start-up processes of a multi-feed well, based loosely on KJ-11, was given. This demonstrated the ability of the simulator to model periods of intense flashing in the well and the resulting fast transients in saturation, pressure and mass flow. Finally, some future applications of transient well models were briefly discussed.

The development of this wellbore simulator is ongoing. This includes investigating the impact on two-phase transient flow of different constitutive equations, particularly those governing slip and friction. Currently, this simulator models the reservoir using simple productivity relationships. Improving the representation of the reservoir, using either radial flow equations or by coupling the wellbore to a numerical reservoir simulator, is required to deal with the future wellbore modelling challenges discussed above.

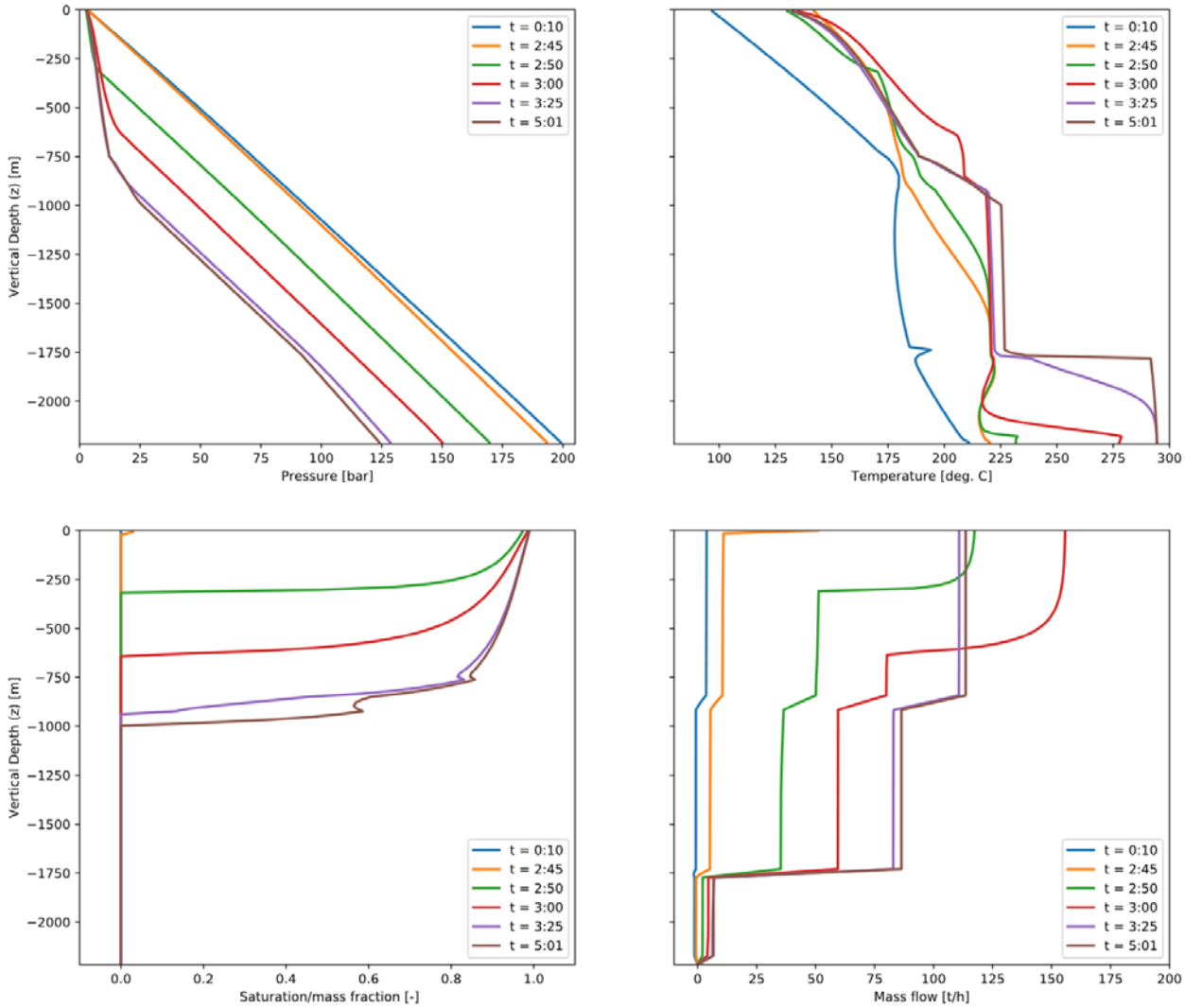

Figure 10: Simulated profiles for pressure, temperature, saturation and mass flow during the start-up of the wellbore described in Section 5.

REFERENCES

Akbar, S., Fathianpour, N. and Al-Khoury, R.: A finite element model for high enthalpy two-phase flow in geothermal wellbores, *Renewable Energy*, 94. (2016).

Axelsson, G.: Geothermal Well testing, *Short Course V on Conceptual Modelling of Geothermal Systems*. (2013).

Aunzo, Z. P., Bjornsson, G. and Bodvarsson, G. S.: *Wellbore Models GWELL, GWNACL, and HOLA User's Guide*. (1991).

Beattie, D.: A Note on the Calculation of Two-Phase Pressure Losses, *Nuclear Engineering and Design*, 25. (1973).

Bjornsson, G.: *A Multi-Feedzone Geothermal Wellbore Simulator*. University of California, Berkeley. (1987).

Chiu, K. and Thakur, S. C.: Modeling of Wellbore Heat Losses in Directional Wells under Changing Injection Conditions, *SPE Annual Technical Conference and Exhibition 1991*. pp. 517-528. (1991).

Chisholm, D.: Pressure gradients due to friction during the flow of evaporating two-phase mixtures in smooth tubes and channels, *International Journal of Heat and Mass Transfer*, 16. pp. 347–358. (1973).

García-Valladares, O., Sánchez-Upton, P. and Santoyo, E.: Numerical modeling of flow processes inside geothermal wells: An approach for predicting production characteristics with uncertainties, *Energy Conversion and Management*. pp. 1621-1643. (2006).

Gudmundsdottir, H. and Jonsson, M. T.: The Wellbore Simulator FloWell – Model Enhancement and Verification, *Proc. World Geothermal Congress 2015*, Melbourne, AUS. (2015).

Freeston, D. H. and Gunn, C. 'Wellbore Simulation - Case Studies', in *Proc. 18th Workshop on Geothermal Reservoir Engineering Stanford University*, Stanford.. (1993).

Horne, R. N. and Shinohara, K.: Wellbore Heat Loss in Production and Injection Wells, *J Pet Technol*, 31. (1979).

Itoi, R., Katayama, Y., Tanaka, T., Kumagai, N. and Iwasaki, T.: Numerical Simulation of Instability of Geothermal Production Well, *Geothermal Resource Counsel Transactions*, 37. pp. 837–842. (2013).

Khasani, Jalilinasrabady, S., Fujii, H. and Itoi, R.: Numerical study on the effects of wellhead restriction modes on the transient behaviours of a geothermal well deliverability applicable for short period of measurement, *Geothermics*, 69. pp. 34–44. (2017).

Bendiksen, K. H., Maines, D., Moe, R., & Nuland, S.: The Dynamic Two-Fluid Model OLGA: Theory and Application. *SPE Production Engineering*, *6*(02), (1991).

Marquez, S., Sazon, T. and Omagbon, J.: SIMGWEL : EDC's New Geothermal Wellbore Modeling Software, *Proc. World Geothermal Congress 2015*, Melbourne., Australia (2015).

Mcguinness, M. J.: SwelFlo User Manual, NZ. (2015).

Miller, C.: *Wellbore User's Manual*, University of California, Berkeley, CA. (1980).

Miller, C.: Wellbore Storage Effects in Geothermal Wells, *Society of Petroleum Engineers Journal*. (1980).

Miller, C., Benson, S., O'Sullivan, M. and Pruess, K.: Wellbore Effects in the Analysis of Two-Phase Geothermal Well Tests. *Society of Petroleum Engineers Journal*, 22. pp. 309–320. (1982).

Ortiz-Ramirez, J.: Two-Phase Flow in Geothermal Wells: Development and Uses of a Computer Code. (1983).

Pan, L. Freifeld, B. Doughty, C., Zakem, S., Sheu, M., Cutright, B. and Terrall, T.: Fully coupled wellbore-reservoir modeling of geothermal heat extraction using CO2 as the working fluid, *Geothermics*, 53. (2015).

Pan, L. and Oldenburg, C. M.: T2Well - An integrated wellbore-reservoir simulator, *Computers and Geosciences*, 65. pp. 46–55. (2014).

Pan, L., Webb, S. W. and Oldenburg, C. M.: Analytical solution for two-phase flow in a wellbore using the drift-flux model, *Advances in Water Resources*, 34. (2011).

Ramey, H. J.: Wellbore Heat Transmission, *Journal of Petroleum Technology*, 14. pp. 427–435. (1962).

Shi, H. Holmes, J., Durlofsky, L., Aziz, K., Diaz, L., Alkaya, B and Oddie, G.: Drift-Flux Modeling of Two-Phase Flow in Wellbores, *SPE Journal*. Society of Petroleum Engineers, 10. pp. 24–33. (2005).

Tonkin, R. O'Sullivan, J. and O'Sullivan, M. On the Choice of Primary Variables in Geothermal Wellbore modelling. Proc. 42nd New Zealand Geothermal Workshop, Waitangi, NZ. (2020).

Upadhyay, R., Hartz, J., Tomkoria, B. and Gulati, A.: Comparison Of Calculated And Observed Pressure Drops In Geothermal Wells Producing Steam-Water Mixtures. 52nd Annu. Fall Tech. Conf. Exhib. Soc. Pet. Eng. (1977).

Vasini, E., Battistelli, A., Berry, P., Bonduà, S., Bortolotti, V., Cormio, C. and Pan, L.: Interpretation of production tests in geothermal wells with T2Well-EWASG., *Geothermics*, 73. pp. 158–167. (2018).

Vijayan, P. K., Patil, A. P., Pilkhwal, D. S., Saha, D. and Venkat Raj, V.: Assessment of pressure drop and void fraction correlations with data from two-phase natural circulation loops, *Heat and Mass Transfer*, 36. (2000).

Willhite, G. P.: Over-all Heat Transfer Coefficients in Steam And Hot Water Injection Wells, *Journal of Petroleum Technology*, 19. pp. 607–615. (1967).

Yamamura, K., Itoi, R., Tanaka, T. and Iwasaki, T.: Numerical Analysis of Transient Steam-Water Two-Phase Flow in Geothermal Production Wells with Multiple Feed Zones, Proc. 42nd Workshop on Geothermal Reservoir Engineering Stanford University, Stanford, CA. (2017).

Yadigaroglu, G., & Hewitt, G. F. Introduction to Multiphase Flow (G. Yadigaroglu & G. F. Hewitt (eds.)). (2018).

Zarrouk, S. J. and McLean, K.: *Geothermal Well Test Analysis: Fundamentals, Applications and Advanced Techniques*. (2019).

Zuber, N. and Findlay, J. A.: Average Volumetric Concentration in Two-Phase Flow Systems, *Journal of Heat Transfer*. ASME, 87. pp. 453–468. (1965).

ISSN 2703-4275